

Zhenfeng Wang, Wenyuan Wu\*, Xue Bian and Yongfu Wu

# Low temperature green synthesis of $\text{LaAlO}_3$ using microcrystalline $\text{LaOCl}$ and amorphous $\text{Al}_2\text{O}_3$ precursors derived from spray pyrolysis

DOI 10.1515/gps-2016-0087

Received April 18, 2016; accepted August 4, 2016; previously published online September 15, 2016

**Abstract:**  $\text{LaAlO}_3$  was synthesized using microcrystalline  $\text{LaOCl}$  and amorphous  $\text{Al}_2\text{O}_3$  precursors. The precursors were derived with single inorganic materials through spray pyrolysis. The precursors and derived oxide powders were characterized by differential thermal analysis, scanning electron microscopy, X-ray diffraction, and transmission electron microscopy.  $\text{LaAlO}_3$  was found to crystallize directly from microcrystalline  $\text{LaOCl}$  and amorphous  $\text{Al}_2\text{O}_3$  precursors at 1073 K for 2 h in air, and the  $\text{LaAlO}_3$  product purity is more than 99.9%.

**Keywords:** amorphous  $\text{Al}_2\text{O}_3$ ;  $\text{LaAlO}_3$ ; microcrystalline  $\text{LaOCl}$ ; precursor; spray pyrolysis.

## 1 Introduction

$\text{LaAlO}_3$  has attracted attention in recent years due to its varied application.  $\text{LaAlO}_3$  has a rhombohedral structure at room temperature and is usually defined as hexagonal with  $a=5.364 \text{ \AA}$  and  $c=13.11 \text{ \AA}$  [1]. It has good dielectric characteristics, including high relative permittivity ( $\epsilon_r=23$ ), a high quality factor ( $Q \times f \approx 68,000$ ;  $Q=1/\tan\delta$ ;  $f$ , measuring frequency; and  $\tan\delta$ , dissipation factor), and a very small temperature coefficient of resonant frequency ( $\tau_f=-44 \times 10^{-6} \text{ K}$ ) [2], which is compatible with applications in dielectric resonators.  $\text{LaAlO}_3$  has been widely used as a substrate for depositing superconducting thin films for microwave devices because it provides a high quality factor, as well as excellent lattice and thermal expansion

equal to that of Y-Ba-Cu-O and Bi-Sr-Ca-Cu-O superconductors [3, 4]. Due to its high surface area and catalytic activity,  $\text{LaAlO}_3$  has also been used to catalyze the oxidative coupling of methane. It is necessary to reduce the sintering temperatures of  $\text{LaAlO}_3$  ceramics, which are usually in the range of 1673–1873 K, to produce multilayered miniaturized devices because the  $\text{LaAlO}_3$  ceramics must be co-sintered with low-melting conductors. Lowering the sintering temperature can be achieved by using fine particle-sized homogenous powders, as well as the addition of melting glass and ceramic pigments [5, 6].

$\text{LaAlO}_3$  is generally synthesized at temperatures  $>1823 \text{ K}$  via a solid-solid reaction route (conventional mixed oxide synthesis) [7]. This method presents a number of drawbacks, such as high reaction temperature, long soaking time, large particle size, limited chemical homogeneity, and low sinterability. Various low temperature chemical routes have been tried, including the following: co-precipitation [8, 9], emulsion combustion [10], a mechanochemical route [11], citrate combustion [12], and a PVA evaporation route. The major drawback of most of these chemical routes is that they require a variety of inorganic and organic precursors, which adds significant complexity to the process. Spray pyrolysis is a green method for the decomposition of single inorganic precursors in the air. In this method, hydrogen chloride produced by exhaust gas is absorbed directly, which provides advantages including short residence time, high production efficiency, low operating cost, and minimized energy consumption. During the preparation process, atomized droplets of a precursor solution undergo evaporation and shrinkage while flowing through a high-temperature reactor. Eventually, these drop into solid particles. Because evaporation, precipitation, drying, and decomposition all occur in a dispersed phase within a single step, it is possible to control the particle properties (size, morphology, chemical composition, etc.) by controlling the process parameters (residence time and decomposition temperature) [13–17]. Therefore, this method provides a continuous flow process that is greener and more economical than other methods. Lux et al. accomplished the synthesis of aluminate lanthanum by spray pyrolysis with metal nitrate as

\*Corresponding author: Wenyuan Wu, School of Materials and Metallurgy, Northeastern University, Shenyang 110004, China, e-mail: wuw@smm.neu.edu

Zhenfeng Wang and Xue Bian: School of Materials and Metallurgy, Northeastern University, Shenyang, China

Yongfu Wu: School of Materials and Metallurgy, Northeastern University, Shenyang, China; and School of Energy and Environment, Inner Mongolia University of Science and Technology, Baotou, China

the raw material [18]. The method presented here is superior to that described by Byron et al. because metal nitrates are not products from an industrial production line, and Byron et al.'s method requires higher pyrolysis and roasting temperatures of 1773 K and 1373 K, respectively.

In this study, we report an easy, inexpensive, and reliable method to synthesize  $\text{LaAlO}_3$  powders with a high surface area that are crystallized at low temperatures and sintered to near full density. The synthesized precursor and  $\text{LaAlO}_3$  powders have been characterized using powder X-ray diffraction analysis (XRD) and scanning electron microscopy (SEM/EDS). The synthetic mechanism is discussed herein.

## 2 Materials and methods

### 2.1 Microcrystalline $\text{LaOCl}$ and amorphous $\text{Al}_2\text{O}_3$ precursor synthesis

Solutions of  $\text{AlCl}_3 \cdot 6\text{H}_2\text{O}$  and  $\text{LaCl}_3 \cdot 7\text{H}_2\text{O}$  (AR, >99.0%, Sinopharm Chemical Reagent Co. Ltd.) were used as precursors for the  $\text{LaAlO}_3$  powder. The La-containing solution was added to the Al-containing solution in a molar ratio of 1:1. The concentration of the precursors was 20.0 wt%. The schematic representation of the spray pyrolysis equipment (Northeastern University in Shenyang, Liaoning Province, China) is shown in Figure 1. The spray pyrolysis system consisted of a home-made atomizer, a corundum tube located inside a tubular furnace, and three cyclones as the collectors; hydrogen chloride produced by exhaust gas is absorbed directly. Droplet diffused through

the high temperature zone, quickly evaporated, and underwent dehydration, and the resultant pyrolysate was collected by a filter sampler. The temperature of the tubular furnace was controlled and adjusted in the temperature range of 873–1073 K. Particle residence time in the hot zone is controlled by the flow controllers, which corresponds to a residence time of 1.0–2.0 s.

### 2.2 $\text{LaAlO}_3$ synthesis

The reaction between microcrystalline  $\text{LaOCl}$  and amorphous  $\text{Al}_2\text{O}_3$  precursors was complete after roasting at 1073 K for 2 h.

### 2.3 Characterization of prepared particles

The products were determined by a powder XRD (X'Pert Pro, PANalytical Corporation, The Netherlands) with  $\text{Cu K}\alpha$  radiation ( $\lambda = 0.154 \text{ nm}$ ) at 40 kV and 40 mA. The scan rate was  $4^\circ 2\theta \text{ min}^{-1}$ , and the scan ranged from  $10^\circ$  to  $90^\circ 2\theta$ . Peak positions and relative intensities were characterized by comparison with the International Centre for Diffraction Data files. DSC and TGA, respectively, using a Netzsch STA 449 F3 Jupiter apparatus (Netzsch Instruments Inc., Burlington, MA, USA) was equipped with a TASC414/4 controller. DSC/TG measurements were carried out from room temperature to 1273 K at the rate of 10 K/min with air flow. The transmission electron microscope (TEM) examinations were performed using a TEM instrument (Tecnai G220; FEI, Hillsboro, OR, USA) operating at 200 kV. The samples were collected directly onto Cu microgrids, and a droplet of suspending liquid was deposited onto a Cu microgrid and allowed to dry. SEM images were obtained on a Zeiss ULTRA plus SEM (Zeiss Ultra Plus, Zeiss, Oberkochen, Germany) equipped with energy dispersive X-ray spectroscopy (EDS), which was used to observe the SEM microstructure.

## 3 Results and discussion

The  $\text{LaOCl}$  precursor was generated from  $\text{LaCl}_3$  via pyrolysis. The  $\text{Al}_2\text{O}_3$  precursor was generated from  $\text{AlCl}_3$  via pyrolysis. A mixture of  $\text{LaOCl}$  and  $\text{Al}_2\text{O}_3$  was obtained via spray pyrolysis of a mixed solution of  $\text{LaCl}_3$  and  $\text{AlCl}_3$ . This pyrolysis reaction can be expressed as follows:

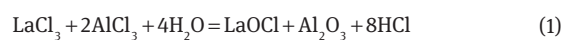
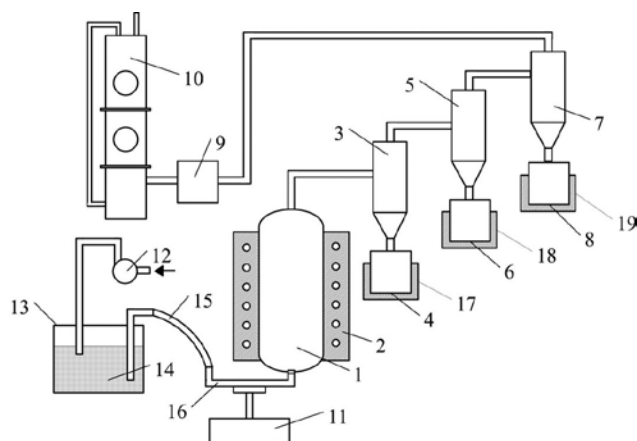
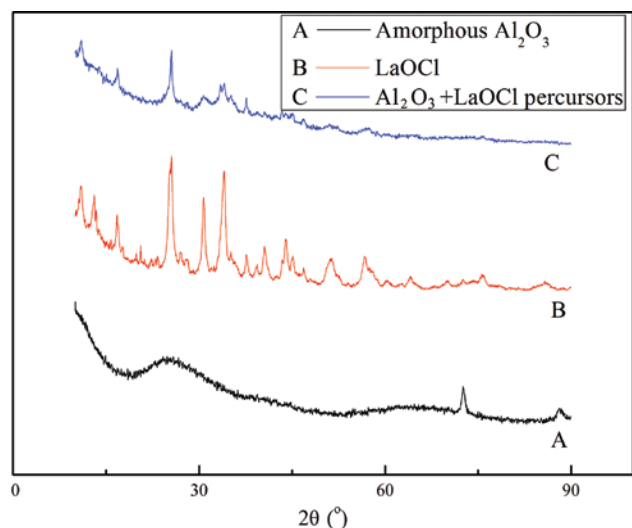


Figure 2 shows the XRD patterns of samples obtained by spray pyrolysis. Figure 2A shows three broad diffuse peaks between diffraction angles  $20^\circ$  and  $70^\circ$ ; the presence of small-shaped peaks indicates that there is a crystalline phase mixed with the primary amorphous structures. Figure 2B presents the XRD patterns of  $\text{LaOCl}$  prepared by spray pyrolysis. The  $\text{LaOCl}$  peaks are observed at  $12.87^\circ$ ,  $25.20^\circ$ ,  $30.70^\circ$ ,  $33.95^\circ$ ,  $43.96^\circ$ , and  $56.68^\circ$ . Peak



**Figure 1:** Schematic diagram of automated spray pyrolysis experimental device. (1) Corundum tube, (2) tubular furnace, (3) the first-stage cyclone, (4) the first stage collector, (5) the second level cyclone separator, (6) the second stage collector, (7) the third cyclone, (8) the third stage collector, (9) flow controllers, (10) tail gas absorber, (11) lifting device, (12) air compressor, (13) tank, (14) solution, (15) hose, (16) injection pipe, (17–19) water bath temperature control.



**Figure 2:** X-ray diffraction patterns of amorphous  $\text{Al}_2\text{O}_3$ , micro crystalline  $\text{LaOCl}$ ,  $\text{Al}_2\text{O}_3$ , and  $\text{LaOCl}$  precursors.

broadening observed in the XRD pattern for  $\text{LaOCl}$  indicates the presence of  $\text{LaOCl}$  crystallites with an average diameter ( $D$ ) of 26.6 nm. Due to the amorphous nature of aluminum oxide, the XRD pattern (Figure 2C) obtained from a mixture of  $\text{Al}_2\text{O}_3$  and  $\text{LaOCl}$  precursors primarily displays  $\text{LaOCl}$  peaks. Figure 3 shows the XRD pattern for the  $\text{LaAlO}_3$  product obtained after roasting at 1073 K for 2 h. The geometry for the product is rhombohedral based upon the calculated XRD patterns.

TG and DTA were measured to study the endothermic and exothermic effects of  $\text{Al}_2\text{O}_3$  and  $\text{LaOCl}$  precursors, and the respective curves are shown in Figure 4. Three weight loss steps were observed in the TGA curve. The first weight

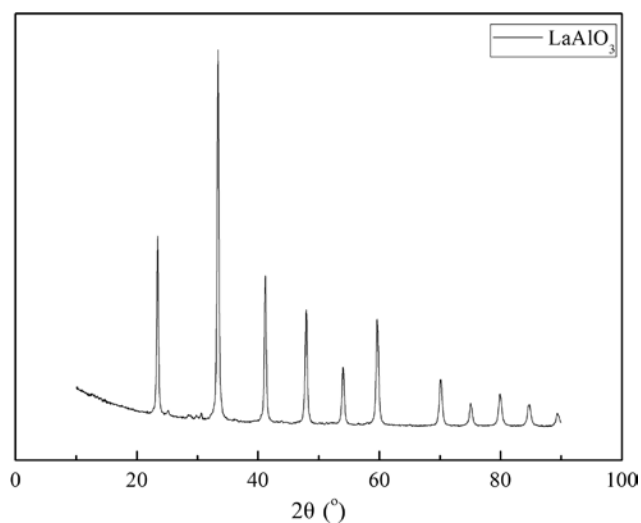


**Figure 3:** X-ray diffraction patterns of  $\text{LaAlO}_3$ .

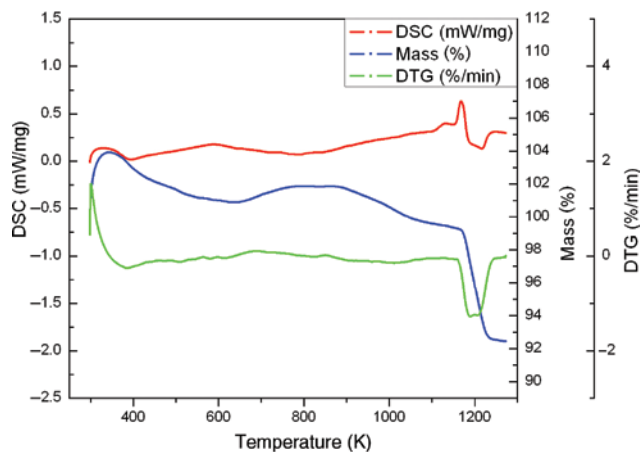


**Figure 4:** TGA, DTG, and DTA curves for the precursors powder.

loss between 300 and 500 K in the TGA curve is due to the desorption of physically absorbed water. The second sharp weight loss step between 880 and 1070 K corresponds to the crystallization processes of amorphous  $\text{Al}_2\text{O}_3$  into the  $\gamma\text{-Al}_2\text{O}_3$  crystallization processes. The third weight loss step between 1070 and 1270 K corresponds to the reaction of  $\text{Al}_2\text{O}_3$  with  $\text{LaOCl}$  to generate  $\text{LaAlO}_3$ . An obvious weight loss appeared at 1160 K; this is explained by an increase in temperature increasing the intensity of the reaction.

Figure 5A and B shows TEM micrographs and SAED patterns of amorphous  $\text{Al}_2\text{O}_3$ . The diffraction pattern shows an amorphous ring, which is consistent with the conclusion that alumina crystals did not grow. The mean diameter of the nanoparticles was 20 and 100 nm for  $\text{LaOCl}$ , respectively (Figure 5C and D). From the larger size particle dark field TEM image (Figure 5D) can be found that the particles are composed of a plurality of small grain aggregates. So these values are consistent with the XRD results. The particles of  $\text{Al}_2\text{O}_3$  and  $\text{LaOCl}$  synthesized by spray pyrolysis have a size distribution of 0.5–15.0  $\mu\text{m}$  (Figure 5E). In Figure 5F, the dark field TEM image shows that  $\text{Al}_2\text{O}_3$  and  $\text{LaOCl}$  precursor particles are composed of small grains; energy spectrum analysis of the different positions of the precursor particles, lanthanum, aluminum, chlorine, and oxygen and differences of content show that the reaction of  $\text{Al}_2\text{O}_3$  and  $\text{LaOCl}$  occurs in the grain boundary.

The SEM images and EDS patterns of the  $\text{Al}_2\text{O}_3$  and  $\text{LaOCl}$  precursors are shown in Figure 6. It can be seen from the SEM images (Figure 6A) that the particles comprise hollow spheres or flake particles with a particle size distribution between 0.5 and 15.0  $\mu\text{m}$ . The EDS pattern (Figure 6B) confirms the presence of La, Al, O, and Cl. Figure 6C shows that the  $\text{LaAlO}_3$  powder consists of highly porous agglomerates of round-shaped particles.

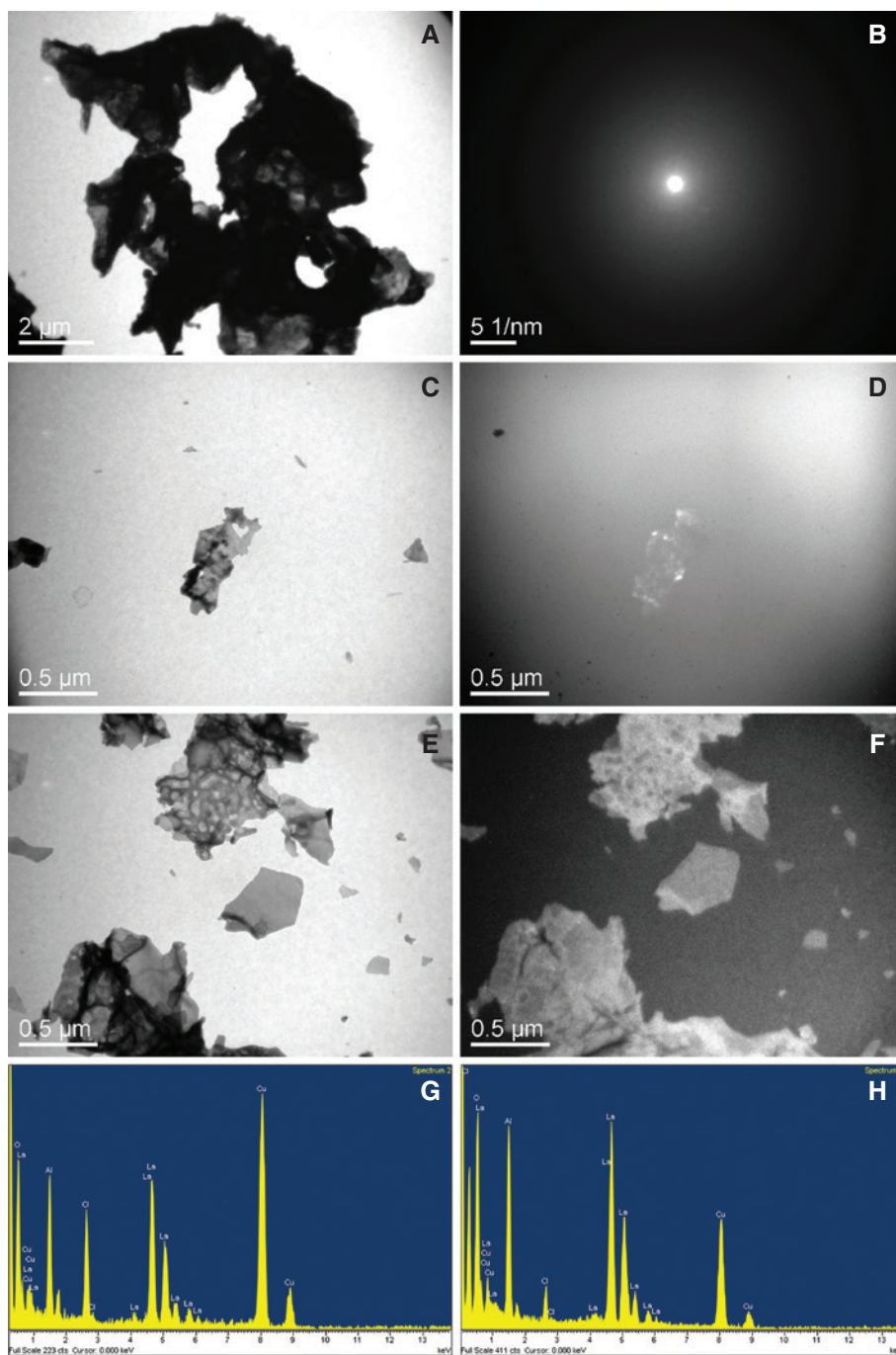


**Figure 5:** TEM images and SAED patterns of the amorphous  $\text{Al}_2\text{O}_3$ , micro crystalline  $\text{LaOCl}$ ,  $\text{Al}_2\text{O}_3$ , and  $\text{LaOCl}$  precursors.

The porous structure could be caused by the large volume of gases ( $\text{Cl}_2$ ) released during the reaction. On the other hand, the round shape of the particles might be related to the presence of precursors, which melt during the reaction process and forces  $\text{LaAlO}_3$  particles to adopt a spherical shape. This type of particle morphology had a positive influence during the pressing and sintering stage. The EDS (Figure 6D) pattern confirms the presence of La, Al, and O in the sample.

## 4 Conclusion

Thermodynamic calculations reveal that the initial reaction temperature of  $\text{LaOCl}$  and  $\text{Al}_2\text{O}_3$  is 2244K. This synthesis method provides  $\text{LaAlO}_3$  powders from metal chlorides at remarkably low temperatures (1073 K). This method has several advantages over existing techniques: (1) with metal chloride as raw materials, the vast majority of rare



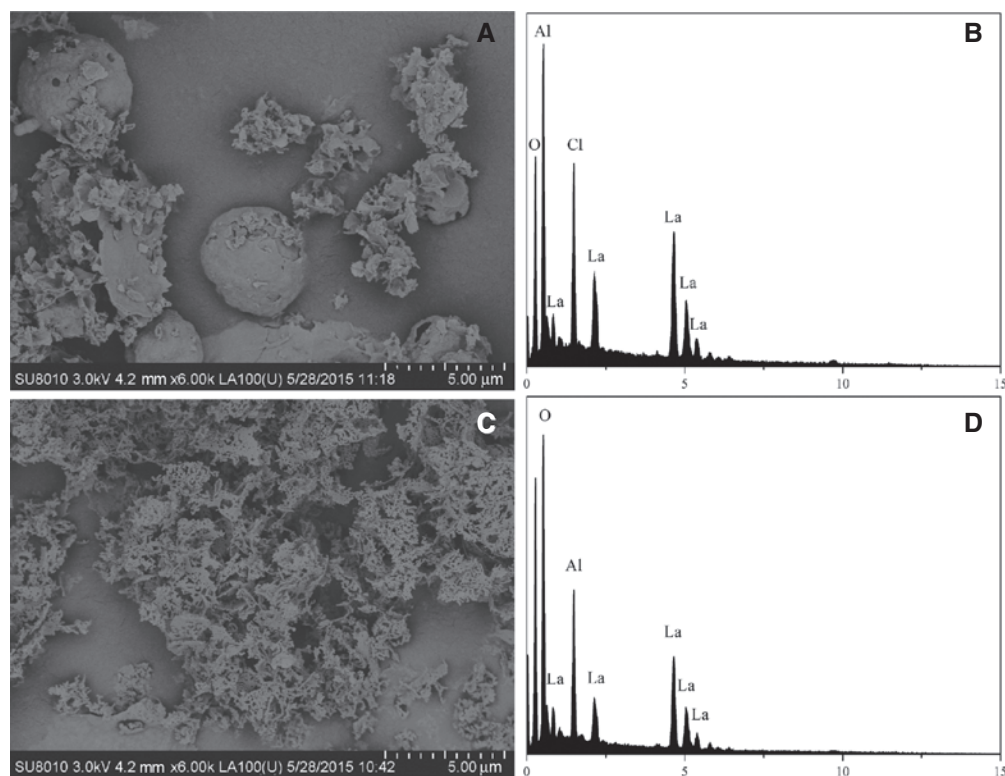


**Figure 6:** SEM images and EDS patterns of the  $\text{Al}_2\text{O}_3$  and  $\text{LaOCl}$  precursors,  $\text{LaAlO}_3$  product.

earth products common to industrial production exists in the form of rare earth chloride and fluoride; (2) compared with other low temperature syntheses, spray pyrolysis is a greener method, which occurs via decomposition of single inorganic materials (metal chloride) in air; and (3) the  $\text{LaAlO}_3$  purity was more than 99.9%, as confirmed through measurements of chloride ion content.

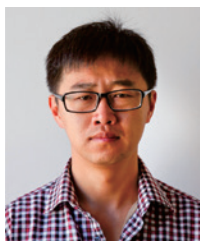
The XRD, TEM, and SAED methods showed that the precursors synthesized by spray pyrolysis were microcrystalline  $\text{LaOCl}$  and amorphous  $\text{Al}_2\text{O}_3$ . These particular forms of the precursors were achieved at significantly lower reaction temperatures. Using this method, perovskite structure compounds  $\text{LaCrO}_3$  and  $\text{LaCoO}_3$  were also successfully synthesized.

**Acknowledgments:** This work was financially supported by the National Natural Science Foundation of China (51274060).

## References

- [1] Lee JJ, Park YS, Yang CS, Kim HS, Kim KH, Kang KY, Kang TW, Park SH, Lee JY. *J. Cryst. Growth*, 2000, 213, 33–39.
- [2] Cho SY, Kim IT, Hong KS. *J. Mater. Res.* 1999, 14, 114–119.
- [3] Simon RW, Platt CE, Lee AE, Lee GS, Daly KP, Wire MS, Luine JA, Urbanik M. *Appl. Phys. Lett.* 1988, 53, 2677–2679.
- [4] Sandu V, Jaklovszky J, Miu D, Drăgulescu D, Grigoriu C, Bunescu MC. *J. Mater. Sci. Lett.* 1994, 13, 1222–1225.
- [5] Sahu PK, Behera SK, Pratihari SK, Bhattacharyya S. *Ceram. Int.* 2004, 30, 1231–1235.
- [6] Ianoș R, Lazău R, Borcănescu S, Băbuță R. *Ceram. Int.* 2014, 40, 7561–7565.
- [7] Li Z, Zhang S, Lee WE. *J. Eur. Ceram. Soc.* 2007, 27, 3201–3205.
- [8] Robert P, Seisenbaeva GA, Wiglusz RJ, Leszek K, Kessler VG. *Inorg. Chem.* 2011, 50, 2966–2974.
- [9] Behera SK, Sahu PK, Pratihari SK, Bhattacharyya S. *Mater. Lett.* 2004, 58, 3710–3715.
- [10] Chandradass J, Kim KH. *J. Alloys Compd.* 2009, 481, L31–L34.
- [11] Zhang Q, Saito F. *J. Am. Ceram. Soc.* 2000, 83, 439–441.
- [12] Adak AK, Pramanik P. *Mater. Lett.* 1997, 30, 269–273.
- [13] Castañeda L, Alonso JC, Ortiz A, Andrade E, Saniger JM, Bañuelos JG. *Mater. Chem. Phys.* 2003, 77, 938–944.
- [14] Fukui T, Ohara S, Naito M, Nogi K. *J. Eur. Ceram. Soc.* 2003, 23, 2963–2967.
- [15] Ibáñez RL, Barrado JRR, Martín F, Brucker F, Leinen D. *Surf. Coat. Technol.* 2004, s188–189, 675–83.
- [16] Martín MI, Rabanal ME, Gómez LS, Torralba JM, Milosevic O. *J. Eur. Ceram. Soc.* 2008, 28, 2487–2494.
- [17] Vallet-Regí M, Rodríguez-Lorenzo LM, Ragel CV, Salinas AJ, González-Calbet JM. *Solid State Ionics* 1997, 101, 197–203.
- [18] Lux BC, Clark RD, Salazar A, Sveum LK, Krebs MA. *J. Am. Ceram. Soc.* 1993, 76, 2669–2672.

## Bionotes



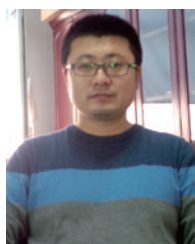
**Zhenfeng Wang**

Zhenfeng Wang is a PhD student at Northeastern University, China. His primary research interests include rare earth chloride and aluminum chloride spray pyrolysis and preparation of rare earth oxide materials.



**Wen Yuan Wu**

Wen Yuan Wu is a professor and PhD supervisor at Northeastern University. His research interests include hydrometallurgy and precious metals metallurgy technology and application.



**Xue Bian**

Xue Bian is an associate professor and a Master's supervisor at Northeastern University. His research interests include rare metal metallurgical technology and application, comprehensive utilization of green technology, rare earth resources, green preparation technology, and rare earth materials.



**Yongfu Wu**

Yongfu Wu is a PhD student at Northeastern University, China, and an associate professor and Master's supervisor at Inner Mongolia University of Science and Technology. His research interests include rare earth metallurgy process simulation and optimization.